Apparatus-dependent corrections to the electron $g-2$ revisited

Ulrich D. Jentschura
Department of Physics and LAMOR, Missouri University of Science and Technology, Rolla, Missouri 65409, USA

(Received 1 January 2023; accepted 14 March 2023; published 19 April 2023)

We revisit the derivation of the apparatus-dependent correction to the energy levels of quantum cyclotron states, as previously outlined [Boulware *et al.*, Phys. Rev. D **32**, 729 (1985)]. We evaluate the leading corrections to the axial, magnetron, cyclotron, and spin-projection-dependent energy levels due to the altered photon field quantization in the vicinity of a conducting wall. Our work significantly extends previous considerations. Quantum cyclotron states are used for the determination of the electron g factor in Penning traps. Our calculations show that the numerically largest apparatus-dependent corrections can be expected for the axial and magnetron frequencies, where they can be as large as 10^{-8} in relative units. For the cyclotron frequency, one can expect corrections on the order of 10^{-12}, which can affect the determination of the anomalous magnetic moment of the electron.

DOI: 10.1103/PhysRevD.107.076014

I. INTRODUCTION

Current g factor measurements are carried out in Penning traps [1–6], not in empty space. The measurements aim to determine the g factor of the free (unbound) electron to utmost precision. Yet, in an actual measurement, the trapped electron is in a bound state (a quantum cyclotron state), and, moreover, its radiation field is subject to the boundary conditions set by the walls of the trap. The uniform magnetic and the quadrupole electric fields of the Penning trap confine the quantum orbit of the electron to a region whose spatial dimension (in the direction perpendicular to the magnetic field of the trap) is of the order of the quantum cyclotron Bohr radius

$$a_{0,c} = \sqrt{\frac{\hbar}{m\omega_c}}. \tag{1}$$

Here, $\omega_c = |e|B_{\rm T}/m$ is the cyclotron frequency, which we assume to be larger than the magnetron and axial frequencies of the Penning trap. The electron mass is denoted as m, while the uniform magnetic field of the Penning trap is denoted as $\vec{B}_{\rm T}$, and its modulus is $B_{\rm T} = |\vec{B}_{\rm T}|$. (One usually assumes that it is directed along the z axis, but, in the current context, we reserve the z axis for a different symmetry in the problem.)

In the direction parallel to the magnetic field of the trap, the quantum orbit of the bound electron is confined to a region commensurate with the axial Bohr radius

$$a_{0,z} = \sqrt{\frac{\hbar}{m\omega_z}}, \tag{2}$$

where ω_z is the resonance frequency of the harmonic oscillator corresponding to the axial, confining, quadrupole electric field of the trap.

On the classical level, corrections to the motion of the electron inside the trap due to mirror charges have been discussed in Ref. [2]. These calculations, however, do not include effects mediated by field quantization. Notably, the perturbation of the quantum electrodynamic self-energy of the bound electron due to apparatus-induced effects has been discussed in Ref. [7]. For completeness, we should point out the existence of alternative treatments (e.g., Ref. [8]). It turns out that subtle considerations related to the choice of gauge for the vector potential corresponding to the magnetic trapping field [9] invalidate the analysis leading to a previously claimed, numerically large effect [8]. The preferred treatment available in the literature, which takes into account the quantum cyclotron wave functions and energy levels, is Ref. [2]. Here, we extend the treatment outlined in Ref. [7] to include the apparatus-dependent correction to the axial frequency and the spin-flip frequency. Subleading corrections to the cyclotron frequency are also analyzed. In comparison to the full Penning trap geometry, we here simplify the situation somewhat and consider, just as in Ref. [2], the electron to be in the vicinity of a perfectly conducting wall, which is assumed to be located in the xy plane.

This paper is organized as follows. In Sec. II, we lay the foundations for the later analysis by recalling the quantum cyclotron wave functions (Sec. II A), the definition of the photon propagator (Sec. II B), and the environment-induced corrections to the photon propagator in the vicinity of a conducting wall (Sec. II C). The apparatus-dependent correction to the photon propagator is discussed in Sec. III.

In Sec. III A, we find a useful representation of the correction to the self-energy of the electron bound in a quantum cyclotron state in Eq. (26). Corrections to cyclotron and axial frequencies are discussed in Sec. III B, while the treatment of the spin-flip frequency is reserved for Sec. III C. Conclusions are drawn in Sec. IV. From now on, we use natural units with $\hbar = c = \epsilon_0 = 1$.

II. QUANTUM CYCLOTRON AND PHOTON PROPAGATOR

A. Minireview on quantum cyclotron states

In order to understand the quantum cyclotron levels inside a Penning trap, it is, first of all, necessary to remember that the kinetic momentum is given by

$$\vec{\pi}_{\rm T} = \vec{p} - e\vec{A}_{\rm T} = \vec{p} - \frac{e}{2}(\vec{B}_{\rm T} \times \vec{r}), \tag{3}$$

where $\vec{B}_{\rm T} = B_{\rm T}\hat{e}_z$ is the magnetic field in the trap and $\vec{p} = -i\vec{\nabla}$ is the kinetic momentum operator. We temporarily assume, for definiteness, that the magnetic field of the trap is directed along the z axis, which is also the axis of the electric quadrupole potential. The variable $\vec{r}$ measures the distance to the origin of the coordinate system, which is chosen to coincide with the center of the quantum-mechanical probability density; i.e., in the sense of Eq. (10), one has $\langle\psi_{k\ell ns}|\vec{r}|\psi_{k\ell ns}\rangle = \vec{0}$. The kinetic momentum $\vec{\pi}_{\rm T}$ enters the velocity-gauge interaction Hamiltonian describing the coupling of the bound electron (inside the Penning trap) to the quantized electromagnetic field.

The quadrupole electric field in the trap is attractive along the z axis and repulsive in the xy plane:

$$V = V_z + V_\parallel, \qquad \vec{\nabla}^2 V = 0, \tag{4a}$$

$$V_z = \frac{1}{2}m\omega_z^2 z^2, \qquad V_\parallel = -\frac{1}{4}m\omega_z^2\rho^2. \tag{4b}$$

The unperturbed Hamiltonian is given as follows:

$$H_0 = \frac{(\vec{\sigma}\cdot\vec{\pi}_{\rm T})^2}{2m} + V - \frac{e}{2m}\kappa\vec{\sigma}\cdot\vec{B}_{\rm T}. \tag{5}$$

Eigenfunctions of the unperturbed Hamiltonian H_0 are described [10] by four quantum numbers: the axial quantum number k, the magnetron quantum number ℓ, the cyclotron quantum number n, and the spin projection quantum number $s = \pm 1$. These take on the following values: $k = 0, 1, 2, \ldots$ (axial), $\ell = 0, 1, 2, \ldots$ (magnetron), $n = 0, 1, 2, \ldots$ (cyclotron), and $s = \pm 1$ (spin). We recall, from Ref. [11], the energy eigenvalues of H_0:

$$E_{k\ell ns} = \omega_c(1+\kappa)\frac{s}{2} + \omega_{(+)}\left(n+\frac{1}{2}\right) + \omega_z\left(k+\frac{1}{2}\right) - \omega_{(-)}\left(\ell+\frac{1}{2}\right). \tag{6}$$

It is of note that, in view of the repulsive character of the quadrupole potential, these eigenvalues are not bounded from below. From Ref. [11], we recall the definitions for $\omega_{(+)}$, which is the generalized cyclotron frequency, and $\omega_{(-)}$, which is the generalized magnetron frequency:

$$\omega_{(+)} = \frac{1}{2}\left(\omega_c + \sqrt{\omega_c^2 - 2\omega_z^2}\right) \approx \omega_c, \tag{7}$$

$$\omega_{(-)} = \frac{1}{2}\left(\omega_c - \sqrt{\omega_c^2 - 2\omega_z^2}\right) \approx \frac{\omega_z^2}{2\omega_c}. \tag{8}$$

Matrix elements of the kinetic momentum operators can be evaluated by expressing the Cartesian momentum operator components of the kinetic "trap" momentum $\pi_{\rm T}^i$ in terms of raising and lowering operators of the magnetron, cyclotron, and axial motions. The algebra becomes rather involved.

For reference, we may express some examples for the matrix elements as follows:

$$\langle\pi_{\rm T}^i\pi_{\rm T}^j\rangle = (\delta^{ij} - \hat{B}_{\rm T}^i\hat{B}_{\rm T}^j)P_1 + \hat{B}_{\rm T}^i\hat{B}_{\rm T}^j P_2 + i\epsilon^{ijk}\hat{B}_{\rm T}^k P_3, \tag{9a}$$

$$P_1 = \frac{(3n-k+1)\omega_{(+)}m}{4} + \frac{(n-3k-1)\omega_{(-)}m}{4} + \frac{(n+k+1)\omega_c^2 m}{4(\omega_{(+)}-\omega_{(-)})} \approx \left(n+\frac{1}{2}\right)\omega_c m, \tag{9b}$$

$$P_2 = \left(k+\frac{1}{2}\right)\omega_z m, \qquad P_3 = -\frac{i}{2}m\omega_c. \tag{9c}$$

The structure of the results reflects the fact that the quantum numbers of the virtual states contributing to the matrix elements differ by at most unity from those of the reference state. (As pointed out in Sec. II A, one can express the momentum and position operators as linear combinations of raising and lowering operators for the cyclotron, magnetron, and axial motions.) The above approximation for P_1 is obtained in the limit $\omega_z \to 0$, $\omega_{(-)} \to 0$, and $\omega_{(+)} \to \omega_c$. We use the conventions of Refs. [10,11], for the cyclotron lowering and raising operators $a_{(+)}$ and $a_{(+)}^\dagger$, the axial lowering and raising operators a_z and $a_z^\dagger$, and the magnetron lowering and raising operators $a_{(-)}$ and $a_{(-)}^\dagger$. Kinetic momentum operators, and position operators, can be expressed in terms of linear combinations of the raising and lowering operators [10,11].

The eigenfunctions of the unperturbed Hamiltonian are given as follows:

$$\psi_{k\ell ns}(\vec{r}) = \frac{(a_{(+)}^\dagger)^n}{\sqrt{n!}}\frac{(a_z^\dagger)^k}{\sqrt{k!}}\frac{(a_{(-)}^\dagger)^\ell}{\sqrt{\ell!}}\psi_0(\vec{r})\chi_{s/2}, \qquad \chi_{+1} = \begin{pmatrix}1\\0\end{pmatrix}, \qquad \chi_{-1} = \begin{pmatrix}0\\1\end{pmatrix}. \tag{10}$$

The spin-up ($s = +1$) and spin-down ($s = -1$) ground-state wave functions are given as follows:

$$\psi_{000\pm1}(\vec{r}) = \sqrt{\frac{m\sqrt{\omega_c^2 - 2\omega_z^2}}{2\pi}} \exp\left(-\frac{m}{4}\sqrt{\omega_c^2 - 2\omega_z^2}\,\rho^2\right) \times \left(\frac{m\omega_z}{\pi}\right)^{1/4} \exp\left(-\frac{1}{2}m\omega_z z^2\right)\chi_{\pm1}. \quad (11)$$

The spin-up sublevel of the nth cyclotron ground state and the spin-down sublevel of the $(n+1)$st excited cyclotron state are quasidegenerate and of interest for spectroscopy and determination of the anomalous magnetic moment of the electron [1–4]. For typical trap parameters, the spatial extent of the quantum cyclotron wave function along the magnetic-field axis extends over the micrometer range, while a strong magnetic trapping field confines the quantum motion in the plane perpendicular to the magnetic-field axis, here assumed to be the xy plane, to the range of about 10 nm (see Figs. 1 and 2).

For absolute clarity, we should stress that the treatment outlined in the current "minireview" section assumes that the magnetic field is oriented along the z axis. For the remainder of this article, however, this assumption is being relaxed, and we calculate with an arbitrary axis for the magnetic trap field, defined by the unit vector $\hat{B}_T$. In the following, the conducting wall will be assumed to be (strictly) oriented in the xy plane, so that the distance vector from the conducting wall to the center of the quantum cyclotron state is oriented along the z axis. This assumption also underlies the formulas for the correction to the photon propagator induced by the wall, which is outlined in Sec. II C.

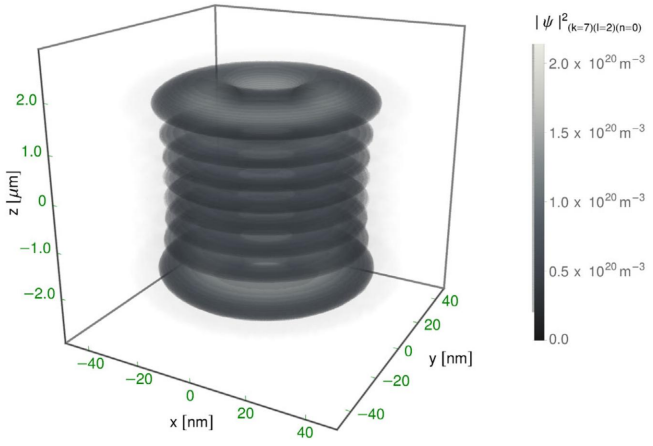

FIG. 1. Using parameters from Ref. [10], $\omega_c = 2\pi \times 164.4$ GHz, $\omega_z = 2\pi \times 64.42$ MHz, and $\omega_{(-)} = 2\pi \times 12.62$ kHz, we calculate the probability density $|\psi|^2 = |\psi_{k\ell ns}(\vec{r})|^2$ of the quantum cyclotron state with quantum numbers $k = 7$, $n = 0$, and $\ell = 2$ [see Eq. (10)]. The quantum numbers describe the seventh axial excited state ($k = 7$), the cyclotron ground state ($n = 0$), and the second excited magnetron state ($\ell = 2$). Of course, per Eq. (10), the probability density remains independent of the spin projection s. The spatial extent of the probability density in the xy plane and in the z direction is commensurate with the generalized Bohr radii, which are (for the given parameters) equal to $a_{0,c} = \sqrt{\hbar/(m\omega_c)} = 10.6$ nm (cyclotron) and $a_{0,z} = \sqrt{\hbar/(m\omega_z)} = 0.435$ μm (axial). Note that, in the plot, we have assumed the magnetic field of the Penning trap to be directed along the z axis.

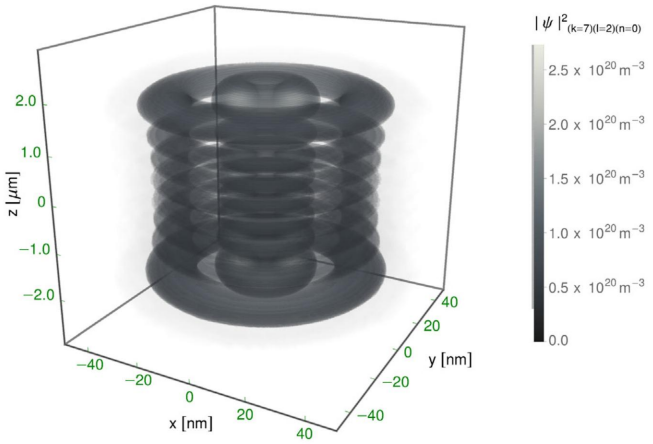

FIG. 2. The same as Fig. 1, but for the state with quantum numbers $k = 7$, $n = 1$, and $\ell = 2$ [see Eq. (10)]. As compared to the state with $n = 0$, one has a more complicated structure of the wave function in the xy plane, due to the excited cyclotron motion.

B. Definition of the photon propagator

Before we discuss details, let us briefly mention a notational dilemma: Namely, the photon wave vector is usually denoted as $\vec{k}$ in the literature (see, e.g., Ref. [12]); yet, the axial quantum number for a quantum cyclotron state is denoted as k, which could very easily be confused with the modulus of the wave vector. One might consider changing the notation for either quantity in the current investigation; however, this would lead to a clash with the existing literature. Hence, we here keep the vector character of the photon wave vector $\vec{k}$ in all formulas and denote its modulus by $|\vec{k}|$, so that we can reserve k for the axial quantum number. Thus, we use the notation $k \neq |\vec{k}|$ throughout this article.

For the later calculations, it helps to write the photon propagator in the vicinity of the wall in a specific representation. For the spatial components ($i, j = 1, 2, 3$) of the unperturbed photon propagator (free boundary conditions), in Coulomb gauge, we use the representation

$$\mathcal{D}^{ij}(\omega, \vec{r}, \vec{r}\,') = \int_0^\infty \mathrm{d}(|\vec{k}|^2)\, \frac{d^{ij}(|\vec{k}|, \vec{r}, \vec{r}\,')}{\vec{k}^2 - \omega^2 - \mathrm{i}\epsilon} = \int \frac{\mathrm{d}^3k}{(2\pi)^3}\, \delta^{\perp,ij}(\vec{k})\, \frac{\mathrm{e}^{\mathrm{i}\vec{k}\cdot(\vec{r}-\vec{r}\,')}}{\vec{k}^2 - \omega^2 - \mathrm{i}\epsilon}, \quad (12)$$

where $d\Omega_k$ is the infinitesimal solid angle of the $\vec{k}$ vector,

$$d^{ij}(|\vec{k}|,\vec{r},\vec{r}') = \frac{|\vec{k}|}{2}\int \frac{d\Omega_k}{(2\pi)^3} e^{i\vec{k}\cdot(\vec{r}-\vec{r}')}\delta^{\perp,ij}(\vec{k}), \quad (13)$$

and

$$\delta^{\perp,ij}(\vec{k}) = \delta^{ij} - \frac{k^i k^j}{\vec{k}^2}. \quad (14)$$

This convention differs by a relative minus sign from the ones used in Eq. (9.72) in Ref. [12] and is in agreement with the ones used in Eq. (1.10) in Ref. [7]. The correction $\delta\mathcal{D}^{ij}$ due to the conducting wall, assumed to be located in the xy plane, ensures that the tangential components of the electric field vanish at the boundary. It can be written as follows:

$$\begin{aligned}\delta\mathcal{D}^{ij}(\omega,\vec{\rho},\vec{\rho}') &= \int_0^\infty d(|\vec{k}|^2)\frac{\delta d^{ij}(|\vec{k}|,\vec{\rho},\vec{\rho}')}{\vec{k}^2-\omega^2-i\epsilon} \\ &= -\int \frac{d^3k}{(2\pi)^3} t^{\perp,ij}(\vec{k})\frac{e^{i\vec{k}\cdot\vec{\rho}-i\vec{k}\cdot\vec{\rho}'}}{\vec{k}^2-\omega^2-i\epsilon}, \quad (15)\end{aligned}$$

where

$$\delta d^{ij}(|\vec{k}|,\vec{\rho},\vec{\rho}') = -\frac{|\vec{k}|}{2}\int \frac{d\Omega_k}{(2\pi)^3} e^{i\vec{k}\cdot\vec{\rho}-i\vec{q}\cdot\vec{\rho}'} t^{\perp,ij}(\vec{k}). \quad (16)$$

The conventions for the involved momentum vectors are as follows:

$$\vec{q} = \{k^x, k^y, -k^z\} = \{k^1, k^2, -k^3\}, \quad (17a)$$

$$q^i = k^i - 2k^3\delta^{i3}, \quad (17b)$$

$$t^{\perp,ij}(\vec{k}) = \delta^{ij} - 2\hat{R}^i\hat{R}^j - \frac{k^i q^j}{|\vec{k}|^2}, \qquad \hat{R}^i = \delta^{i3}. \quad (17c)$$

We have the relations $k^i t^{\perp,ij}(\vec{k}) = t^{\perp,ij}(\vec{k})q^j = 0$. The environment-induced correction (15) is no longer translation invariant, which raises the question of the precise definition of the origin of the coordinate system. The formulas (15) and (16) are valid provided we define the origin of the coordinate system to be the point in the xy plane (the plane of the conducting wall) located directly under the center of the quantum cyclotron wave function. [This is in contrast to the coordinate $\vec{r}$ used in Eq. (3), whose origin is defined to coincide with the center of the probability density of the quantum cyclotron wave function; we assume the origin of the coordinate system to lie in the plane of the conducting wall for the remainder of this article.] This implies, in particular, that the vector $\vec{R}$ from the conducting plate to the center of the quantum cyclotron state has only a z component, $\vec{R} = R\hat{e}_z$. The expression for $\delta\mathcal{D}^{ij}$ follows from the representation for $\mathcal{D}^{ij}$ by the replacement $d^{ij} \to \delta d^{ij}$.

C. Corrections to the photon propagator

For later calculations, we will need the photon propagator and its gradient for equal arguments $\vec{r} = \vec{r}' = \vec{R}$, where $\vec{R} = z\hat{e}_z$ is the position above the conducting wall. In particular, we need a result for the following expression (where we assume that $\vec{R} = R\hat{R} = R\hat{e}_z$):

$$\delta\mathcal{D}^{ij}(\omega,\vec{R},\vec{R}) = -\int \frac{d^3k}{(2\pi)^3} e^{2ik^3R}\frac{t^{\perp,ij}(\vec{k})}{\vec{k}^2-\omega^2-i\epsilon}, \quad (18)$$

where q_ℓ is defined according to Eq. (17a). One uses the relation $d^3k = \frac{1}{2}d\Omega_k d(|\vec{k}|^2)|\vec{k}|$, performs a partial-fraction decomposition of the expression $1/(\vec{k}^2-\omega^2-i\epsilon)$, and uses the symmetry of the resulting integrand under the substitution $k \to -k$, changing the integration interval to $(-\infty,\infty)$. The result is, after some algebra,

$$\begin{aligned}\delta\mathcal{D}^{ij}(\omega,\vec{R},\vec{R}) &= -(\delta^{ij}-\hat{R}^i\hat{R}^j)\frac{\exp(2i|\omega|R)}{8\pi R} \\ &\quad\times\left(1+\frac{i}{2|\omega|R}-\frac{1}{4(|\omega|R)^2}\right) \\ &\quad-\hat{R}^i\hat{R}^j\left(-i\frac{\exp(2i|\omega|R)}{8\pi R(|\omega|R)}\right)\left(1+\frac{i}{2|\omega|R}\right), \\ |\omega| &= \sqrt{\omega^2+i\epsilon}. \quad (19)\end{aligned}$$

The expression $|\omega|$ is the modulus of the photon frequency, defined so that $\mathrm{Im}|\omega|$, i.e., assuming that the branch cut of the square root function is along the positive real axis [13,14]. In particular, the zz component ($i = 3$, $j = 3$) is

$$\begin{aligned}\delta\mathcal{D}^{33}(\omega,\vec{R},\vec{R}) &= \int \frac{d^3k}{(2\pi)^3} e^{2i|\vec{k}|R\cos\theta}\frac{1-\cos^2\theta_k}{\vec{k}^2-\omega^2-i\epsilon} \\ &= \left(-i\frac{\exp(2i|\omega|R)}{8\pi R(|\omega|R)}\right)\left(1+\frac{i}{2|\omega|R}\right), \quad (20)\end{aligned}$$

where θ_k is the polar angle of $\vec{k}$ ($k^3 = k\cos\theta_k$). Note that, in Ref. [7], the term δD^{33} was neglected based on the argument [see the text following Eq. (A7) in Ref. [7]] that, since D^{33} involves the factor $1-\cos^2\theta_k$, it should be smaller asymptotically than the δD^{11} and δD^{22} terms. However, a closer inspection, described in detail below, reveals that the result for δD^{33}, in fact, eventually yields the dominant apparatus-dependent radiative correction to the energy spectrum of the quantum cyclotron levels, expressed in terms of the axial frequency (see also Ref. [15]).

In the leading order in the $1/R$ expansion, the result (19) is in agreement with Eq. (A9) in Ref. [7]:

$$\delta D_{ij} \approx -(\delta^{ij} - \hat{R}^i \hat{R}^j) \frac{e^{2i|\omega|R}}{4\pi(2R)}. \tag{21}$$

Note that the result given in Eq. (19) is not equal to the classical, retarded result for the Green function (see Chap. 2 in Ref. [16]); namely, the ω in the classical result needs to be replaced by $|\omega|$.

III. APPARATUS-DEPENDENT SELF-ENERGY

A. Exploration and useful representation

The interaction Hamiltonian of the electron bound in a quantum cyclotron level to the quantized electromagnetic field, described by the vector potential $\vec{A}$ *of the quantized field* (see Chap. 2 in Ref. [12]), is expressed as

$$H_I = -\frac{e}{2m}(\vec{\pi}_{\rm T} \cdot \vec{A} + \vec{A} \cdot \vec{\pi}_{\rm T}), \tag{22}$$

$$\vec{\pi}_{\rm T} = \vec{p} - e\vec{A}_{\rm T} = \vec{p} - \frac{e}{2}(\vec{B}_{\rm T} \times \vec{r}), \tag{23}$$

where $\vec{\pi}_{\rm T}$ is the kinetic momentum for the trapped electron and $\vec{A}_{\rm T}$ is the vector potential of the trap field. As outlined in Sec. II A, quantum cyclotron states are described by the axial ($k = 0, 1, 2, \ldots$), magnetron ($\ell = 0, 1, 2, \ldots$), cyclotron ($n = 0, 1, 2, \ldots$), and spin ($s = \pm 1$) quantum numbers. The bound-state energies are denoted as $E = E_{k\ell ns}$.

In order to discuss the environment-induced correction to the quantum cyclotron energy levels, we need a convenient representation for the (nonrelativistic) self-energy of these states. This is because the exchange of hard virtual photons with an energy on the order of the electron mass scale is not influenced by the environmental conditions, and, in turn, for the discussion of infrared photons, a nonrelativistic approximation is sufficient (see also Chap. 4 in Ref. [12]). Let us see if the following general *ansatz* for the self-energy and its correction makes sense:

$$\begin{aligned} E_{\rm SE} &= -\sum_{k'\ell'n's'} \frac{e^2}{m^2} \int_0^K {\rm d}|\vec{k}| \int {\rm d}^3 r \int {\rm d}^3 r' \\ &\quad \times \frac{[\psi^\dagger_{k\ell ns}(\vec{r}) \pi^i_{\rm T} \psi_{k'\ell'n's'}(\vec{r})][\psi^\dagger_{k'\ell'n's'}(\vec{r}') \pi'^i_{\rm T} \psi_{k\ell ns}(\vec{r}')]}{E_{k'\ell'n's'} - E_{k\ell ns} + |\vec{k}| - i\epsilon} \\ &\quad \times d^{ij}(|\vec{k}|, \vec{R} + \vec{r}, \vec{R} + \vec{r}') \\ &\approx -\frac{e^2}{m^2} \int {\rm d}k \left\langle \pi^i_{\rm T} \frac{1}{H_0 - E_0 + |\vec{k}| - i\epsilon} \pi^j_{\rm T} \right\rangle \\ &\quad \times d^{ij}(|\vec{k}|, \vec{R}, \vec{R}). \end{aligned} \tag{24}$$

One sums over all possible virtual quantum cyclotron states, which carry the primed quantum numbers k', ℓ', n', and s'. Furthermore, H_0 is the unperturbed Hamiltonian for the electron inside the Penning trap, as defined in Eq. (5). The expression $E_0 = E_{k\ell ns}$ is a shorthand notation for the energy of the reference state. Furthermore, K is an ultraviolet cutoff parameter for the virtual photon momentum which is matched with the infrared divergent slope of the Dirac F_1 form factor of the electron [12,17–19]. For the environment-induced correction, we can replace $K \to \infty$ in view of ultraviolet convergence.

Here, the expression after the first equal sign is approximated by the expression after the second equal sign, replacing $d^{ij}(|\vec{k}|, \vec{R} + \vec{r}, \vec{R} + \vec{r}') \to d^{ij}(|\vec{k}|, \vec{R}, \vec{R})$. For the unperturbed self-energy, this replacement corresponds to the dipole approximation [12]. In view of the translation invariance of the unperturbed photon propagator, one might otherwise set $\vec{R} = \vec{0}$. (This is different for the apparatus-induced correction, which is manifestly not translation invariant.) The operator $\pi'^i_{\rm T} = -i\vec{\nabla}' - e\vec{A}_{\rm T}(\vec{r}')$ in Eq. (24) acts on the primed coordinate $\vec{r}'$. One takes note of the fact that, in bra-ket notation, $\int {\rm d}^3 r' \psi^\dagger_{k'\ell'n's'}(\vec{r}') \pi'^i_{\rm T} \psi_{k\ell ns}(\vec{r}') = \langle k'\ell'n's'|\pi^i_{\rm T}|k\ell ns\rangle$. However, the presence of the term $d^{ij}(|\vec{k}|, \vec{r}, \vec{r}')$ in the integrand in Eq. (24) prevents one from simplifying the integrand unless one replaces $d^{ij}(|\vec{k}|, \vec{r}, \vec{r}') \to d^{ij}(|\vec{k}|, \vec{R}, \vec{R})$.

In summary, we use the convention that unprimed quantum numbers denote the reference state, while primed quantum numbers denote the virtual state. The expression after the first equal sign in Eq. (24) serves as a definition of the expression after the second equal sign. We use the convention that $\pi'^i_{\rm T} = -i\vec{\nabla}' - (e/2)(\vec{B} \times \vec{r}')$ is the kinetic momentum operator with respect to the primed coordinate.

The unperturbed self-energy (without the wall) for an electron bound is found to be

$$\begin{aligned} E_{\rm SE} &= -\frac{e^2}{m^2} \int {\rm d}^3 r \int {\rm d}^3 r' \int {\rm d}|\vec{k}| d^{ij}(|\vec{k}|, \vec{R} + \vec{r}, \vec{R} + \vec{r}') \\ &\quad \times \left\langle \pi^i_{\rm T} \frac{1}{H_0 - E_0 + |\vec{k}| - i\epsilon} \pi'^j_{\rm T} \right\rangle \\ &\approx -\frac{e^2}{m^2} \int {\rm d}|\vec{k}| \left\langle \pi^i_{\rm T} \frac{1}{H_0 - E_0 + |\vec{k}| - i\epsilon} \pi^j_{\rm T} \right\rangle \\ &\quad \times \frac{|\vec{k}|}{2} \int \frac{{\rm d}\Omega_k}{(2\pi)^3} \left(\delta^{ij} - \frac{k^i k^j}{\vec{k}^2} \right) \\ &= \frac{2\alpha}{3\pi} \int {\rm d}|\vec{k}| |\vec{k}| \left\langle \frac{\pi^i_{\rm T}}{m} \frac{1}{E_0 - H_0 - |\vec{k}| + i\epsilon} \frac{\pi^i_{\rm T}}{m} \right\rangle. \end{aligned} \tag{25}$$

In the second step, we have employed the dipole approximation and have replaced a factor $e^{i\vec{k}\cdot(\vec{r}-\vec{r}')}$ by unity. The final expression in Eq. (25) is precisely the result we would otherwise obtain from a Bethe logarithm calculation (see Chap. 4 in Ref. [12]).

Eventually, Eq. (24) describes the low-energy part of the self-energy, which is due to low-energy virtual

photons—those with an energy of the order of the atomic binding or of the binding energy inside the Penning trap. The idea is that the dominant correction due to the modified boundary conditions could, in principle, influence only low-energy (long-wavelength) photons. Hence, as we replace $d^{ij}(|\vec{k}|,\vec{R}+\vec{r},\vec{R}+\vec{r}') \to \delta d^{ij}(|\vec{k}|,\vec{R}+\vec{r},\vec{R}+\vec{r}')$, we can hope that we obtain ultraviolet convergent expressions which do not require additional renormalizations. In view of the above considerations, the apparatus-induced correction to the Bethe logarithm is finally found to be

$$\begin{aligned}\delta E_{\rm SE} &= -\sum_{k'\ell'n's'} \frac{e^2}{m^2} \int {\rm d}|\vec{k}| \int {\rm d}^3 r \int {\rm d}^3 r' \\ &\quad \times \frac{[\psi^\dagger_{k\ell ns}(\vec{r})\pi^i_{\rm T}\psi_{k'\ell'n's'}(\vec{r})][\psi^\dagger_{k'\ell'n's'}(\vec{r}')\pi'^i_{\rm T}\psi_{k\ell ns}(\vec{r}')]}{E_{k'\ell'n's'} - E_{k\ell ns} + |\vec{k}| - {\rm i}\epsilon} \\ &\quad \times \delta d^{ij}(|\vec{k}|,\vec{R}+\vec{r},\vec{R}+\vec{r}') \\ &\approx -\frac{e^2}{m^2} \int {\rm d}|\vec{k}| \left\langle \pi^i_{\rm T} \frac{1}{H_0 - E_0 + |\vec{k}| - {\rm i}\epsilon} \pi^j_{\rm T} \right\rangle \\ &\quad \times \delta d^{ij}(|\vec{k}|,\vec{R},\vec{R}). \end{aligned} \tag{26}$$

The theoretical errors induced by the replacement $d^{ij}(|\vec{k}|,\vec{R}+\vec{r},\vec{R}+\vec{r}') \to \delta d^{ij}(|\vec{k}|,\vec{R}+\vec{r},\vec{R}+\vec{r}')$ are of the order of $a_{0,c}/R$ and $a_{0,z}/R$ [where the generalized Bohr radii are defined in Eqs. (1) and (2)]. In view of typical trap parameters (see also Figs. 1 and 2), with the trap dimensions being in the centimeter range [10], the error induced by the approximation $d^{ij}(|\vec{k}|,\vec{R}+\vec{r},\vec{R}+\vec{r}') \approx d^{ij}(|\vec{k}|,\vec{R},\vec{R})$ is less than one percent for the results reported below (which pertain to small environment-induced effects anyways).

B. Corrections to cyclotron and axial frequencies

In order to evaluate the correction listed in Eq. (26), one expresses the momentum operators in the matrix element $\langle \pi^i_{\rm T}[1/(H_0 - E_0 + |\vec{k}| - {\rm i}\epsilon)]\pi^j_{\rm T}\rangle$ in terms of raising and lowering operators of the cyclotron, magnetron, and axial motions. One then obtains, from the propagator denominators, expressions of the functional form $[1/(|\vec{k}| + \omega - {\rm i}\epsilon)] + 1/(|\vec{k}| - \omega - {\rm i}\epsilon)]$, where ω can be the cyclotron or the axial frequency. Let us derive an important intermediate relation ($\epsilon \to 0^+$):

$$\frac{1}{|\vec{k}| + \omega - {\rm i}\epsilon} + \frac{1}{|\vec{k}| - \omega - {\rm i}\epsilon} = \frac{2|\vec{k}|}{\vec{k}^2 - \omega^2 - {\rm i}\epsilon} + \mathcal{O}(\epsilon). \tag{27}$$

The last of the mentioned steps involves a redefinition of ϵ. In fact, ϵ is redefined as a quantity multiplied by k in the second line. The infinitesimal imaginary part in the expression after the equal sign in Eq. (27) is written in such a way that it displays symmetry under the replacement $|\vec{k}| \to -|\vec{k}|$. This symmetrization is useful because one can then extend the integration interval from $|\vec{k}| \in (0,\infty)$ to $|\vec{k}| \in (-\infty,\infty)$ and use the Cauchy residue theorem. After writing the kinetic momentum operators in terms of raising and lowering operators for the magnetron, cyclotron, and axial motions and using Eq. (27) repeatedly, one obtains the result

$$\begin{aligned}\left\langle \pi^i_{\rm T} \frac{1}{H_0 - E_0 + |\vec{k}| - {\rm i}\epsilon} \pi^j_{\rm T} \right\rangle &\approx (\delta^{ij} - \hat{B}^i_{\rm T}\hat{B}^j_{\rm T}) \left(\frac{|\vec{k}|(n+\frac{1}{2})\omega_c m}{\vec{k}^2 - \omega_c^2 - {\rm i}\epsilon} - \frac{\frac{1}{2}m\omega_c^2}{\vec{k}^2 - \omega_c^2 - {\rm i}\epsilon} \right) \\ &\quad + (\delta^{ij} - \hat{B}^i_{\rm T}\hat{B}^j_{\rm T}) \left(\frac{|\vec{k}|(\ell+\frac{1}{2})\frac{\omega_{(-)}^2}{\omega_c} m}{\vec{k}^2 - \omega_{(-)}^2 - {\rm i}\epsilon} + \frac{\frac{1}{2}\frac{\omega_{(-)}^3}{\omega_c} m}{\vec{k}^2 - \omega_{(-)}^2 - {\rm i}\epsilon} \right) + \hat{B}^i_{\rm T}\hat{B}^j_{\rm T} \left(\frac{|\vec{k}|(k+\frac{1}{2})\omega_z m}{\vec{k}^2 - \omega_z^2 - {\rm i}\epsilon} - \frac{\frac{1}{2}m\omega_z^2}{\vec{k}^2 - \omega_z^2 - {\rm i}\epsilon} \right) \\ &\quad + {\rm i}\epsilon^{ijk}\hat{B}^k_{\rm T} \left(\frac{(n+\frac{1}{2})\omega_c^2 m}{\vec{k}^2 - \omega_c^2 - {\rm i}\epsilon} - \frac{\frac{1}{2}|\vec{k}|\omega_c m}{\vec{k}^2 - \omega_c^2 - {\rm i}\epsilon)} + \frac{(\ell+\frac{1}{2})\frac{\omega_{(-)}^3}{\omega_c} m}{\vec{k}^2 - \omega_c^2 - {\rm i}\epsilon} + \frac{\frac{1}{2}|\vec{k}|\frac{\omega_{(-)}^2}{\omega_c} m}{\vec{k}^2 - \omega_c^2 - {\rm i}\epsilon} \right), \end{aligned} \tag{28}$$

where $k \neq |\vec{k}|$ is the axial quantum number. The structure of these results is again reminiscent of Eq. (9). Furthermore, in the term proportional to $(\delta^{ij} - \hat{B}^i_{\rm T}\hat{B}^j_{\rm T})$, we have kept the leading terms in the limits $\omega_z \to 0$, $\omega_{(-)} \to 0$, and $\omega_{(+)} \to \omega_c$. The term proportional to $\epsilon^{ijk}\hat{B}^k_{\rm T}$ vanishes after multiplication with the photon propagator. Terms that uniformly shift all quantum cyclotron levels do not lead to physically observable effects and can be ignored in Eq. (28).

One decisive observation makes the calculation of the environment-induced correction to the quantum cyclotron energy levels easier: Namely, the quantities $\delta\mathcal{D}^{ij}$ and δd^{ij} are related by an equation involving an integral over ${\rm d}(|\vec{k}|^2)$ and a weighting factor $1/(\vec{k}^2 - \omega^2 - {\rm i}\epsilon)$. Yet, the result (28) contains terms of the $k/(\vec{k}^2 - \omega^2 - {\rm i}\epsilon)$, where $\omega = \omega_c$, $\omega = \omega_{(-)}$, and $\omega = \omega_z$. When combined with the integral operator $\int {\rm d}k$, expressions are obtained which exactly lead back to $\delta\mathcal{D}^{ij}$.

The induced correction to the self-energy is, with the help of Eqs. (19), (26), and (28),

$$\begin{aligned}\delta E_{\rm SE} \approx& -\frac{e^2}{m}\left(\frac{1}{2}\int_0^\infty \frac{{\rm d}(|\vec{k}|^2)}{\vec{k}^2-\omega_c^2-{\rm i}\epsilon}\right)\delta d^{ij}(k,\vec{R},\vec{R})(\delta^{ij}-\hat{B}^i_{\rm T}\hat{B}^j_{\rm T})\left(n+\frac{1}{2}\right)\omega_c\\ &-\frac{e^2}{m}\left(\frac{1}{2}\int_0^\infty \frac{{\rm d}(|\vec{k}|^2)}{\vec{k}^2-\omega_c^2-{\rm i}\epsilon}\right)\delta d^{ij}(k,\vec{R},\vec{R})\hat{B}^i_{\rm T}\hat{B}^j_{\rm T}\left(k+\frac{1}{2}\right)\omega_z\\ \approx& -\frac{e^2}{2m}\delta\mathcal{D}^{ij}(\omega_c,\vec{R},\vec{R})(\delta^{ij}-\hat{B}^i_{\rm T}\hat{B}^j_{\rm T})\left(n+\frac{1}{2}\right)\omega_c\\ &-\frac{e^2}{2m}\delta\mathcal{D}^{ij}(\omega_{(-)},\vec{R},\vec{R})(\delta^{ij}-\hat{B}^i_{\rm T}\hat{B}^j_{\rm T})\left(\ell+\frac{1}{2}\right)\frac{\omega_{(-)}^2}{\omega_c}\\ &-\frac{e^2}{2m}\delta\mathcal{D}^{ij}(\omega_z,\vec{R},\vec{R})\hat{B}^i_{\rm T}\hat{B}^j_{\rm T}\left(k+\frac{1}{2}\right)\omega_z. \end{aligned} \tag{29}$$

With the help of results of the form $(\delta^{ij}-\hat{R}^i\hat{R}^j)(\delta^{ij}-\hat{B}^i_{\rm T}\hat{B}^j_{\rm T})=1+(\hat{R}\cdot\hat{B}_{\rm T})^2$, one obtains the final result as

$$\begin{aligned}\delta E_{\rm SE} =& \frac{r_0}{4R}{\rm e}^{2{\rm i}\omega_z R}\left[1+\frac{3{\rm i}}{2\omega_z R}-\frac{3}{4(\omega_z R)^2}+(\hat{R}\cdot\hat{B}_{\rm T})^2\left\{1-\frac{\rm i}{2\omega_z R}+\frac{1}{4(\omega_z R)^2}\right\}\right]\left(n+\frac{1}{2}\right)\omega_c\\ &+\frac{r_0}{4R}{\rm e}^{2{\rm i}\omega_{(-)}R}\left[1+\frac{3{\rm i}}{2\omega_{(-)}R}-\frac{3}{4(\omega_{(-)}R)^2}+(\hat{R}\cdot\hat{B}_{\rm T})^2\left\{1-\frac{\rm i}{2\omega_{(-)}R}+\frac{1}{4(\omega_{(-)}R)^2}\right\}\right]\left(\ell+\frac{1}{2}\right)\frac{\omega_{(-)}^2}{\omega_c}\\ &+\frac{r_0}{4R}{\rm e}^{2{\rm i}\omega_z R}\left[1+\frac{\rm i}{2\omega_z R}-\frac{1}{4(\omega_z R)^2}-(\hat{R}\cdot\hat{B}_{\rm T})^2\left\{1-\frac{\rm i}{2\omega_z R}+\frac{1}{4(\omega_z R)^2}\right\}\right]\left(k+\frac{1}{2}\right)\omega_z. \end{aligned} \tag{30}$$

We use the fact that $r_0=e^2/(4\pi m)=2.8\times10^{-13}$ cm is the classical electron radius. The above result is more complicated, and more complete, than the result recorded in Eq. (1.4) in Ref. [7]. In particular, the numerically large correction to the axial frequency is being included. One uses the fact that, for typical trap geometries, one has

$$\omega_c R\gg 1, \qquad \omega_z R\ll 1, \qquad \omega_{(-)}R\ll 1. \tag{31}$$

Isolating the leading terms in the above limits and taking the real part of the energy shift, one obtains

$$\begin{aligned}\delta E_{\rm SE} \approx& \frac{r_0}{4R}\cos(2\omega_c R)[1+(\hat{R}\cdot\hat{B}_{\rm T})^2]\omega_c\left(n+\frac{1}{2}\right)\\ &+\frac{r_0}{16\omega_{(-)}\omega_c R^3}[(\hat{R}\cdot\hat{B}_{\rm T})^2-3]\omega_{(-)}\left(\ell+\frac{1}{2}\right)\\ &+\frac{r_0}{16\omega_z^2 R^3}[1+(\hat{R}\cdot\hat{B}_{\rm T})^2]\omega_z\left(k+\frac{1}{2}\right). \end{aligned} \tag{32}$$

The result given in Eq. (2.7) in Ref. [7] contains the first term on the right-hand side of Eq. (32). The results in Eq. (32) are written so that the relative corrections to the unperturbed spectrum (6) can be readily identified.

C. Corrections to the spin-flip frequency

In order to obtain the spin-dependent correction to the self-energy, one needs to generalize the transition current to include the magnetic interaction. This can be done by considering Eqs. (11.111) and (11.115) in Ref. [12]:

$$\vec{j}=\frac{\vec{\pi}_{\rm T}}{m}+\frac{1+\kappa}{2m}\vec{\sigma}\times\vec{\nabla}, \tag{33}$$

where the $\vec{\nabla}$ operator acts on the photon vector potential field operator and $\kappa\approx\alpha/(2\pi)$ is the anomalous magnetic moment correction [20]. The current operator $\vec{j}$ is valid for the annihilation part of the photon vector potential operator. For the creation part, one replaces $\vec{\nabla}\to-\vec{\nabla}$. The self-energy of the quantum cyclotron state, taking into account the generalization of Eq. (26), with the spin-dependent part of the current (33) included, is

$$\begin{aligned}\delta E_\sigma =& -\frac{e^2}{m^2}\int_0^\infty {\rm d}|\vec{k}|\left\langle\left[\pi^i_{\rm T}+(1+\kappa)\frac{(\vec{\sigma}\times\vec{\nabla})^i}{2}\right]\right.\\ &\times\frac{1}{H_0-E_0+|\vec{k}|-{\rm i}\epsilon}\left.\left[\pi^j_{\rm T}-(1+\kappa)\frac{(\vec{\sigma}\times\vec{\nabla}')^j}{2}\right]\right\rangle\\ &\times\delta d^{ij}(|\vec{k}|,\vec{r},\vec{r}')\Big|_{\vec{r}=\vec{r}'=\vec{R}}. \end{aligned} \tag{34}$$

The operators $\vec{\nabla}$ and $\vec{\nabla}'$ act on the photon propagation function $\delta d^{ij}(|\vec{k}|,\vec{r},\vec{r}')$, not on the quantum cyclotron states. We again use the approximation that, after the calculation of the gradient of the photon propagator, we can set $\vec{r}=\vec{r}'=\vec{R}$.

It is possible to obtain an order-of-magnitude estimate of the spin-dependent, environment-induced correction. Namely, the dominant term is obtained when the gradient operator in the current acts on the photon propagation function, which, in turn, contains the factor $\exp(2\mathrm{i}\omega_c R)$ (for virtual transitions that change the cyclotron quantum number). Taking the scaling of the operators as derived in Ref. [11] into account, we have the following order-of-magnitude estimates:

$$\frac{\vec{\pi}_{\mathrm{T}}}{m}\sim\sqrt{\frac{\omega_c}{m}},\qquad \frac{\vec{\sigma}\times\vec{\nabla}}{2m}\sim\frac{\omega_c}{m}. \tag{35}$$

The leading environment-induced correction involves two operators $\vec{\pi}_{\mathrm{T}}/m$ [see Eq. (26)].

The spin-dependent term obtained by replacing one of the convective current operators in Eq. (34) by a spin-dependent current, therefore, constitutes a correction of relative order $\sqrt{\omega_c/m}$. If one replaces both convective current operators by spin-dependent terms, then one obtains a correction of relative order ω_c/m.

From Eq. (34), we derive the term linear in the spin-dependent current, which leads to the first spin-dependent correction $\delta E_{\sigma,\mathrm{lin}}$, as follows:

$$\delta E_{\sigma,\mathrm{lin}}=-\frac{e^2}{2m^2}\int_0^\infty \mathrm{d}|\vec{k}|\left\langle\sigma^k\frac{1}{H_0-E_0+|\vec{k}|-\mathrm{i}\epsilon}\pi_{\mathrm{T}}^j\right\rangle \times(1+\kappa)\epsilon^{ik\ell}\nabla^\ell\delta d^{ij}(|\vec{k}|,\vec{r},\vec{R})|_{\vec{r}=\vec{R}}+\mathrm{H.c.}, \tag{36}$$

where H.c. denotes the Hermitian adjoint. A closer inspection, though, shows that the matrix element in the integrand of Eq. (36) vanishes:

$$\left\langle\sigma^k\frac{1}{H_0-E_0+k-\mathrm{i}\epsilon}\pi_{\mathrm{T}}^j\right\rangle =\sum_{k'\ell'n's'}\frac{\langle k\ell ns|\sigma^k|k'\ell'n's'\rangle\langle k'\ell'n's'|\pi_{\mathrm{T}}^j|k\ell ns\rangle}{E_{q'\ell'n's'}-E_{q\ell ns}+|\vec{k}|-\mathrm{i}\epsilon}=0, \tag{37}$$

and, therefore,

$$\delta E_{\sigma,\mathrm{lin}}=0. \tag{38}$$

The identity (37) can be shown by considering that the spin operator acts only on the spin quantum number s of the reference state, while all Cartesian components of the momentum operator π_{T}^j alter the magnetron, cyclotron, or axial quantum number. Hence, there is no virtual state with quantum numbers $q'\ell'n's'$ which could contribute to the matrix element (37).

The dominant spin-dependent correction is given by the expression

$$\delta E_\sigma=-\frac{e^2}{4m^2}\int_0^\infty \mathrm{d}|\vec{k}|\left\langle\sigma^k\frac{1}{H_0-E_0+|\vec{k}|-\mathrm{i}\epsilon}\sigma^p\right\rangle \times\epsilon^{ik\ell}\epsilon^{jpq}\nabla^\ell\nabla'^q\delta d^{ij}(|\vec{k}|,\vec{r},\vec{r}')\Big|_{\vec{r}=\vec{r}'=\vec{R}}. \tag{39}$$

Based on the order-of-magnitude estimates given in Eq. (35), we can establish that $\frac{\delta E_\sigma}{\delta E_{\mathrm{SE}}}\sim\frac{\omega_c}{m}$; i.e., the spin-dependent part of the apparatus-induced correction is suppressed in comparison to the spin-independent term by an additional factor ω_c/m.

The calculation becomes easier if one considers the difference between spin-up and spin-down states. For an operator M, we denote the spin-dependent difference as

$$\langle\!\langle M\rangle\!\rangle=\langle\psi_{k\ell n(s=1)}|M|\psi_{k\ell n(s=1)}\rangle -\langle\psi_{k\ell n(s=-1)}|M|\psi_{k\ell n(s=-1)}\rangle. \tag{40}$$

After some algebra, one obtains the following result for the spin-dependent matrix element of the propagator:

$$\langle\!\langle\sigma^i\frac{1}{H_0-E_0+|\vec{k}|}\sigma^j\rangle\!\rangle=-(\delta^{ij}-\hat{B}_{\mathrm{T}}^i\hat{B}_{\mathrm{T}}^j)\frac{2\omega_s}{\vec{k}^2-\omega_s^2-\mathrm{i}\epsilon} +\epsilon^{ijk}\hat{B}_{\mathrm{T}}^k\frac{2\mathrm{i}k}{\vec{k}^2-\omega_s^2-\mathrm{i}\epsilon},\qquad \omega_s\equiv(1+\kappa)\omega_c. \tag{41}$$

The spin-flip frequency $\omega_s=\omega_c(1+\kappa)$ is numerically close to the cyclotron frequency ω_c. In the limit $|\omega|R\to\infty$, one obtains the following results for the integral of the gradient of the photon propagation function:

$$\int_0^\infty \mathrm{d}|\vec{k}|\frac{1}{\vec{k}^2-\omega^2-\mathrm{i}\epsilon}\nabla^k\nabla'^\ell\delta d^{ij}(|\vec{k}|,\vec{r},\vec{r}')\Big|_{\vec{r}=\vec{r}'=\vec{R}} \approx-\hat{R}^k\hat{R}^\ell(\delta^{ij}-\hat{R}^i\hat{R}^j)\frac{|\omega|\mathrm{e}^{2\mathrm{i}|\omega|R}}{16\pi R}\left(R\gg\frac{1}{|\omega|}\right). \tag{42}$$

In the long-range limit, the spin-dependent correction is, thus, found as

$$\langle\!\langle\delta E_\sigma\rangle\!\rangle=-\frac{r_0}{8R}\frac{\omega_s}{m}\mathrm{e}^{2\mathrm{i}\omega_s R}(1+(\hat{R}\cdot\hat{B}_{\mathrm{T}})^2)\omega_s +\mathrm{i}\frac{r_0}{16R}\frac{\omega_s}{m}\frac{\mathrm{e}^{2\mathrm{i}\omega_s R}}{\omega_s R}(3-(\hat{R}\cdot\hat{B}_{\mathrm{T}})^2)\omega_s +\mathcal{O}\left(\frac{r_0}{R}\frac{\omega_s}{m}\frac{1}{(\omega_s R)^2}\right),\qquad \omega_s R\to\infty. \tag{43}$$

Again, r_0 is the classical electron radius.

In the short-range limit, the result is more complicated:

$$\langle\langle \delta E_\sigma \rangle\rangle = \frac{r_0}{4\pi m R^2}(1-(\hat{R}\cdot\hat{B}_{\rm T})^2)\omega_s - \frac{r_0}{6\pi m R^2}(\omega_s R)^2\omega_s - \frac{r_0}{\pi m R^2}(\omega_s R)^2(\hat{R}\cdot\hat{B}_{\rm T})^2 \times\left[\frac{2}{3}(\ln(2\omega_s R)+\gamma_E) - \frac{{\rm i}\pi}{3} - \frac{13}{18}\right]\omega_s + \mathcal{O}\left(\frac{r_0}{mR^2}(\omega_s R)^4\omega_s\right), \qquad \omega_s R \to 0. \tag{44}$$

Here, $\gamma_E = 0.55721\ldots$ is the Euler-Mascheroni constant. The complete result, valid for arbitrary distance R, constitutes and interpolating function between the long-range limit (43) and the short-range expression (44) and involves sine and cosine integrals:

$$\begin{aligned}\langle\langle \delta E_\sigma \rangle\rangle = {}& \frac{r_0}{32\pi m R^3}\{2\cos(2\omega_s R)[3\omega_s R\{{\rm Ci}(-2\omega_s R)+{\rm Ci}(2\omega_s R)-2{\rm i}\pi\}+(3-4(\omega_s R)^2){\rm Si}(2\omega_s R)] \\ &+\sin(2\omega_s R)[(-3+4(\omega_s R)^2)\{{\rm Ci}(-2\omega_s R)+{\rm Ci}(2\omega_s R)-2{\rm i}\pi\}+12\omega_s R{\rm Si}(2\omega_s R)]-4\omega_s R\} \\ &+\frac{r_0}{32\pi m R^3}(\hat{R}\cdot\hat{B}_{\rm T})^2\{2\cos(2\omega_s R)[-\omega_s R\{{\rm Ci}(-2\omega_s R)+{\rm Ci}(2\omega_s R)-2{\rm i}\pi\}-(1+(4\omega_s R)^2){\rm Si}(2\omega_s R)] \\ &+\sin(2\omega_s R)[(1+4(\omega_s R)^2)\{{\rm Ci}(-2\omega_s R)+{\rm Ci}(2\omega_s R)-2{\rm i}\pi\}-4\omega_s R{\rm Si}(2\omega_s R)]-4\omega_s R\}.\end{aligned} \tag{45}$$

The cosine and sine integrals fulfill the relations

$${\rm Ci}(z) = -\int_z^\infty {\rm d}t\,\frac{\cos(t)}{t}, \tag{46}$$

$${\rm Si}(z) = \frac{\pi}{2} - \int_z^\infty {\rm d}t\,\frac{\sin(t)}{t}. \tag{47}$$

Let us write the result (43) as a relative correction to the spin-flip frequency and isolate the real part:

$$\frac{\langle\langle \delta E_\sigma \rangle\rangle}{\omega_s} \approx -\frac{r_0}{8R}\frac{\omega_s}{m}\cos(2\omega_c R)(1+(\hat{R}\cdot\hat{B}_{\rm T})^2). \tag{48}$$

In this representation, the suppression of the spin-dependent correction by a relative factor $\omega_s/m \approx \omega_c/m$ in comparison to the result (32) becomes particularly apparent. We remember that $\omega_c \approx \omega_s = \omega_c(1+\kappa)$, where ω_s is the spin-flip frequency and $\kappa \approx \alpha/(2\pi)$ is the anomalous magnetic moment correction.

IV. CONCLUSIONS

We have considered the apparatus-induced quantized-field correction to the electron g factor in the vicinity of a conducting wall. We have argued, with Ref. [7], that the problem has to be considered in terms of the modification of the photon propagator, which enters the calculation of the quantum electrodynamic self-energy of the quantum cyclotron state. We have recalled that quantum cyclotron levels are characterized by four quantum numbers, the axial quantum number k, the magnetron quantum number ℓ, the cyclotron quantum number n, and the spin projection quantum number s. The relevant frequencies have been identified [10] as the axial frequency ω_z, the cyclotron frequency, ω_c, the magnetron frequency $\omega_m \approx \omega_z^2/(2\omega_c)$, the cyclotron frequency ω_c, and the spin-flip frequency $\omega_s \approx \omega_c(1+\kappa)$, where $\kappa \approx \alpha/(2\pi)$ is the electron anomaly. One needs to realize, though, that the "z axis" relevant to the calculation of the axial frequency ω_z is not necessarily equal to the z axis in our calculation. Namely, we have assumed that the conducting wall is oriented in the xy plane, with the origin of the coordinate system chosen to be directly below the center of the quantum cyclotron state wave function. That is to say, the distance vector from the conducting wall to the electron is $\vec{R} = R\hat{e}_z$. The axial frequency, however, is calculated with respect to the axis of the magnetic field $\vec{B}_{\rm T}$ of the Penning trap, which is described by the unit vector $\hat{B}_{\rm T}$. Hence, in our final results we have encountered a lot of occurrences of the scalar product $\vec{R}\cdot\vec{B}_{\rm T}$.

For typical trap geometries [10], the hierarchy of the trap frequencies is $\omega_s \approx \omega_c \gg \omega_z$. The apparatus-induced correction to the energy levels of the quantum cyclotron fulfills $\delta E_z \gg \delta E_c \gg \delta E_s$. Our final results are as follows. From the spin-independent part of the self-energy, we obtain the apparatus-induced correction to the axial energy δE_z and the corresponding correction $\delta\omega_z$ to the axial frequency [see Eq. (30)]:

$$\begin{aligned}\delta E_z &= \delta\omega_z\left(k+\frac{1}{2}\right), \\ \frac{\delta\omega_z}{\omega_z} &= \frac{r_0}{4R}{\rm e}^{2{\rm i}\omega_z R}\left[1+\frac{\rm i}{2\omega_z R}-\frac{1}{4(\omega_z R)^2}\right. \\ &\quad \left.-(\hat{R}\cdot\hat{B}_{\rm T})^2\left\{1-\frac{\rm i}{2\omega_z R}+\frac{1}{4(\omega_z R)^2}\right\}\right].\end{aligned} \tag{49}$$

For the magnetron frequency, one observes that, according to Eq. (6), the unperturbed contribution to the quantum cyclotron energy carries a negative prefactor:

$$\delta E_{(-)} = -\delta\omega_{(-)}\left(k+\frac{1}{2}\right),$$
$$\frac{\delta\omega_{(-)}}{\omega_{(-)}} = -\frac{r_0}{4R}\mathrm{e}^{2\mathrm{i}\omega_{(-)}R}\left[1+\frac{3\mathrm{i}}{2\omega_{(-)}R}-\frac{3}{4(\omega_{(-)}R)^2}\right.$$
$$\left.+(\hat{R}\cdot\hat{B}_{\mathrm{T}})^2\left\{1-\frac{\mathrm{i}}{2\omega_{(-)}R}+\frac{1}{4(\omega_{(-)}R)^2}\right\}\right]\frac{\omega_{(-)}}{\omega_c}. \quad (50)$$

The correction δE_c to the cyclotron energy and the corresponding correction $\delta\omega_c$ to the cyclotron frequency are obtained as follows:

$$\delta E_c = \delta\omega_c\left(n+\frac{1}{2}\right),$$
$$\frac{\delta\omega_c}{\omega_c} = \frac{r_0}{4R}\mathrm{e}^{2\mathrm{i}\omega_c R}\left[1+\frac{3\mathrm{i}}{2\omega_c R}-\frac{3}{4(\omega_c R)^2}\right.$$
$$\left.+(\hat{R}\cdot\hat{B}_{\mathrm{T}})^2\left\{1-\frac{\mathrm{i}}{2\omega_c R}+\frac{1}{4(\omega_c R)^2}\right\}\right]. \quad (51)$$

In the limit $\omega_s R \gg 1$, the leading term of the correction to the spin-flip (Larmor) frequency is found as follows [see Eq. (30)]:

$$\delta E(s=+1)-\delta E(s=-1)=\delta\omega_s, \quad (52a)$$

$$\frac{\delta\omega_s}{\omega_s}\approx -\frac{r_0}{8R}(1+(\hat{R}\cdot\hat{B}_{\mathrm{T}})^2)\frac{\omega_s^2}{m}\mathrm{e}^{2\mathrm{i}\omega_s R}, \quad \omega_s R\gg 1, \quad (52b)$$

where $\omega_s=\omega_c(1+\kappa)$ is the unperturbed spin-flip frequency. The next-to-leading-order term for long range can be found in Eq. (43), the short-range expansion is displayed in Eq. (44), and the complete interpolating formula is found in Eq. (45).

In order to estimate the magnitude of the corrections, we use parameters from Ref. [10], $\omega_c = 2\pi\times 164.4$ GHz, $\omega_z = 2\pi\times 64.42$ MHz, and $\omega_{(-)} = 2\pi\times 12.62$ kHz, as well as $R=(1/3)$ cm (see p. 730 in Ref. [2]). One obtains the following estimates (we assume that $\hat{R}\cdot\hat{B}=1$):

$$\frac{\delta\omega_z}{\omega_z}\sim -5.2\times 10^{-9}, \qquad \frac{\delta\omega_{(-)}}{\omega_{(-)}}\sim 1.1\times 10^{-8}, \quad (53a)$$

$$\frac{\delta\omega_c}{\omega_c}\sim -2.3\times 10^{-13}, \qquad \frac{\delta\omega_s}{\omega_s}\sim -2.8\times 10^{-22}. \quad (53b)$$

In order to put these numbers into context, we should note that the above relative corrections pertain to a geometry with one conducting wall being located in the xy plane at a distance R below the center of the quantum cyclotron orbit. An idealized cubic trap would consist of six idealized conducting walls, so that the above numbers would be multiplied by a factor of $2+4\times\frac{1}{2}=4$. This is because, for four of the six walls, one has $\hat{R}\cdot\hat{B}_{\mathrm{T}}=0$ as opposed to $\hat{R}\cdot\hat{B}_{\mathrm{T}}=1$. Also, we use the idealized assumption of additive corrections. Under these assumptions, the relative correction to the cyclotron frequency potentially becomes as large as 10^{-12} [see also Eq. (55)]. For the modified axial frequency of $\omega_z\approx 114$ MHz and magnetron frequency of $\omega_-\approx 43$ kHz given in Ref. [21], the estimates given in Eq. (51) change to $\delta\omega_z/\omega_z\approx -3.0\times 10^{-9}$ and $\delta\omega_{(-)}/\omega_{(-)}\approx -1.7\times 10^{-9}$, respectively. The apparatus-dependent correction to the axial frequency becomes especially relevant if the cyclotron frequency is determined with the help of the invariance theorem, $\omega_c=\sqrt{\omega_{(+)}^2+\omega_-^2+\omega_z^2}$.

Let us now discuss the signature of the apparatus-induced effects in an experiment. The correction to the spin-flip frequency ω_s, given in Eq. (51), is numerically suppressed in comparison to the results for the corrections to the cyclotron frequency in Eq. (51) and the axial and magnetron frequencies in Eq. (49) by a factor $\omega_s/m\approx\omega_c/m$ and can, thus, be neglected. The correction to the axial and magnetron frequencies, while being numerically large, do not directly enter the determination of the anomalous magnetic moment of the electron. This is different for the correction to the cyclotron frequency, which enters the fundamental relation

$$\kappa=\frac{\omega_s}{\omega_c}-1, \quad (54)$$

that determines the anomalous magnetic moment of the electron. In order to classify matters, it is necessary to observe that the functional form of the result given in Eqs. (51) makes it hard to eliminate the effect from the experimental signal: The apparatus-induced correction to the cyclotron energy is equal to $\delta\omega_c(n+1/2)$, i.e., proportional to the unperturbed term $\omega_c(n+1/2)$, and cannot be eliminated from the experimental signal by an elaborate combination of transitions with different quantum numbers n. All cyclotron levels are affected in the same way, independent of n. Furthermore, and this is an important observation, the functional form of the apparatus-induced correction to the cyclotron frequency is independent of the trap geometry as can be seen from the matrix element (28): The first term on the right-hand side of Eq. (28) is proportional to $(n+1/2)$ and will lead to a uniform $\delta\omega_c$ for all quantum cyclotron levels when combined with the appropriate photon propagator correction δd^{ij} [see Eq. (29)] which depends on the trap geometry. More complicated trap geometries will lead to a more complicated form of δd^{ij}, but the result will still be a uniform correction $\delta\omega_c$ to the cyclotron frequency for all quantum cyclotron levels. The uniform $\delta\omega_c$ depends only on the

geometry of the trap and, of course, on the magnetic field B_T. Or, to put it differently, the degrees of freedom of the trap somehow "decouple" from the correction to the cyclotron frequency, leading to a uniform correction $\delta\omega_c$ for all levels.

The shift $\omega_c \to \omega_c + \delta\omega_c$ leads to an apparatus-dependent anomalous magnetic moment $\kappa + \delta\kappa$, where $\delta\kappa$ is the apparatus-dependent correction, given by the formula

$$\kappa + \delta\kappa = \frac{\omega_s}{\omega_c + \delta\omega_c} - 1 \approx \kappa - \frac{\delta\omega_c}{\omega_c}. \tag{55}$$

For illustration, let us consider the case $\hat{R} \cdot \vec{B}_T = 1$ in Eq. (32), restore SI units, and keep only the leading term for long range:

$$\delta\kappa = -\frac{\delta\omega_c}{\omega_c} \approx -\frac{r_0}{2R}\cos\left(\frac{2|e|B_T R}{mc}\right). \tag{56}$$

The right-hand side shows that the signature of the environment-induced effect would be a small (in this case, for the idealized situation of a conducting wall, cosinusoidal) modification of the anomalous magnetic moment with the strength of the magnetic field of the trap. The order of magnitude of $\delta\kappa$ is given by the ratio of the classical electron radius to the trap dimension $r_0/R \sim 10^{-12}$, for $r_0 = 2.8 \times 10^{-15}$ m and $R = 3 \times 10^{-3}$ m. If we assume, with Ref. [10], that $\omega_c = 2\pi \times 164.4$ GHz and $R = 3 \times 10^{-3}$ m, then $\omega_c R/c \approx 10.33$ is large against unity. This means that, by varying the magnetic field strength of the trap moderately (e.g., by a factor of 2), one could change the argument of the cosine in Eq. (56) by roughly 10, which is (given the trivial inequality $10 > 2\pi$) sufficient to cover a full oscillation period of the cosine, and map out the apparatus-induced correction to the g factor experimentally.

Of course, different trap geometries could easily change the above rough estimates by an order of magnitude upward or downward and modify the functional form expected in Eq. (56) from a cosinusoidal dependence to a more complex functional form (whose form could still be mapped out experimentally by simply varying the strength of the magnetic field of the Penning trap). The general statement is that the signature of the apparatus-induced effect would be a small, but discernible, dependence of the cyclotron frequency, and, thus, of the anomalous magnetic moment, on the magnetic field strength in the trap. As indicated in the discussion surrounding Eq. (51), for typical trap parameters, the apparatus-induced effects should alter the determination of the anomalous magnetic moment at the level of $\delta\kappa \sim 10^{-12}$, plus or minus one order of magnitude. These results can also be relevant to other measurements, notably, g factor measurements of antiparticles [22] and atomic mass measurements in Penning traps [23,24].

ACKNOWLEDGMENTS

The author acknowledges helpful conversations with Professor Gerald Gabrielse and support from the Templeton Foundation (Fundamental Physics Block Grant, Subaward No. 60049570 of Grant ID No. 61039).

[1] L. S. Brown and G. Gabrielse, Precision spectroscopy of a charged particle in an imperfect Penning trap, Phys. Rev. A **25**, 2423(R) (1982).
[2] L. S. Brown, G. Gabrielse, K. Helmerson, and J. Tan, Cyclotron Motion in a Microwave Cavity: Possible Shifts of the Measured Electron g Factor, Phys. Rev. Lett. **55**, 44 (1985).
[3] B. Odom, D. Hanneke, B. D'Urso, and G. Gabrielse, New Measurement of the Electron Magnetic Moment Using a One–Electron Quantum Cyclotron, Phys. Rev. Lett. **97**, 030801 (2006); G. Gabrielse, D. Hanneke, T. Kinoshita, M. Nio, and B. Odom, New Determination of the Fine Structure Constant from the Electron g Value and QED, Phys. Rev. Lett. **97**, 030802 (2006); New Determination of the Fine Structure Constant from the Electron g Value and QED, Phys. Rev. Lett. **99**, 039902(E) (2007).
[4] D. Hanneke, S. Fogwell, and G. Gabrielse, Measurement of the Electron Magnetic Moment and the Fine Structure Constant, Phys. Rev. Lett. **100**, 120801 (2008).
[5] X. Fan and G. Gabrielse, Circumventing Detector Backaction on a Quantum Cyclotron, Phys. Rev. Lett. **126**, 070402 (2021).
[6] X. Fan and G. Gabrielse, Driven one-particle quantum cyclotron, Phys. Rev. A **103**, 022824 (2021).
[7] D. G. Boulware, L. S. Brown, and T. Lee, Apparatus-dependent contributions to $g - 2$?, Phys. Rev. D **32**, 729 (1985).
[8] G. Barton and H. Grotch, Magnetic effects in non-relativistic quantum electrodynamics: Image corrections to the electron moment, J. Phys. A **10**, 1201 (1977).
[9] G. Barton and N. S. J. Fawcett, Quantum electromagnetics of an electron near mirrors, Phys. Rep. **170**, 1 (1988).
[10] L. S. Brown and G. Gabrielse, Geonium theory: Physics of a single electron or ion in a Penning trap, Rev. Mod. Phys. **58**, 233 (1986).
[11] A. Wienczek, C. Moore, and U. D. Jentschura, Foldy–Wouthuysen transformation in strong magnetic fields and relativistic corrections for quantum cyclotron energy levels, Phys. Rev. A **106**, 012816 (2022).
[12] U. D. Jentschura and G. S. Adkins, *Quantum Electrodynamics: Atoms, Lasers and Gravity* (World Scientific, Singapore, 2022).
[13] P. J. Mohr, Self-energy radiative corrections in hydrogen–like systems, Ann. Phys. (N.Y.) **88**, 26 (1974).

[14] P. J. Mohr, Numerical evaluation of the $1S_{1/2}$ radiative level shift, Ann. Phys. (N.Y.) **88**, 52 (1974).
[15] D. G. Boulware and L. S. Brown, Comment on "Mass and Anomalous Magnetic Moment of an Electron between Two Conducting Parallel Plates", Phys. Rev. Lett. **55**, 133 (1985).
[16] U. D. Jentschura, *Advanced Classical Electrodynamics: Green Functions, Regularizations, Multipole Decompositions* (World Scientific, Singapore, 2017).
[17] H. A. Bethe, The electromagnetic shift of energy levels, Phys. Rev. **72**, 339 (1947).
[18] K. Pachucki, Higher-order binding corrections to the Lamb shift, Ann. Phys. (N.Y.) **226**, 1–87 (1993).
[19] U. Jentschura and K. Pachucki, Higher-order binding corrections to the Lamb shift of $2P$ states, Phys. Rev. A **54**, 1853 (1996).
[20] J. Schwinger, On quantum-electrodynamics and the magnetic moment of the electron, Phys. Rev. **73**, 416 (1948).
[21] X. Fan, T. G. Myers, B. A. D. Sukra, and G. Gabrielse, Measurement of the Electron Magnetic Moment, Phys. Rev. Lett. **130**, 071801 (2023).
[22] C. Smorra, S. Sellner, M. J. Borchert, J. A. Harrington, T. Higuchi, H. Nagahama, T. Tanaka, A. Mooser, G. Schneider, M. Bohman, K. Blaum, Y. Matsuda, C. Ospelkaus, W. Quint, J. Walz, Y. Yamazaki, S. Ulmer, and E. G. Myers, A parts-per-billion measurement of the antiproton magnetic moment, Nature (London) **550**, 371 (2017).
[23] E. G. Myers, High-precision atomic mass measurements for fundamental constants, Atoms **7**, 37 (2019).
[24] K. Blaum, S. Eliseev, and S. Sturm, Perspectives on testing fundamental physics with highly charged ions in Penning traps, Quantum Sci. Technol. **6**, 014002 (2021).